Vertically oriented two-dimensional Ruddlesden–Popper phase perovskite passivation layer for efficient and stable inverted perovskite solar cells

Yunseong Choi,‡[a] Donghwan Koo,‡[a] Gyujeong Jeong,[a] Ungsoo Kim,[a] Hyungmin Kim,[a] Fuzhi Huang,*[bc] and Hyesung Park*[a]

[a]Department of Materials Science and Engineering, Graduate School of Semiconductor Materials and Devices Engineering, Perovtronics Research Center, Low Dimensional Carbon Materials Center, Ulsan National Institute of Science and Technology, Ulsan 44919, Republic of Korea.

[b]State Key Laboratory of Advanced Technology for Materials Synthesis and Processing, Wuhan University of Technology, Wuhan, 430070, PR China.

[c]Foshan Xianhu Laboratory of the Advanced Energy Science and Technology Guangdong Laboratory, Foshan, 528216, PR China.

‡These authors contributed equally to this work.

*Corresponding author

E-mail address: hspark@unist.ac.kr, fuzhi.huang@whut.edu.cn

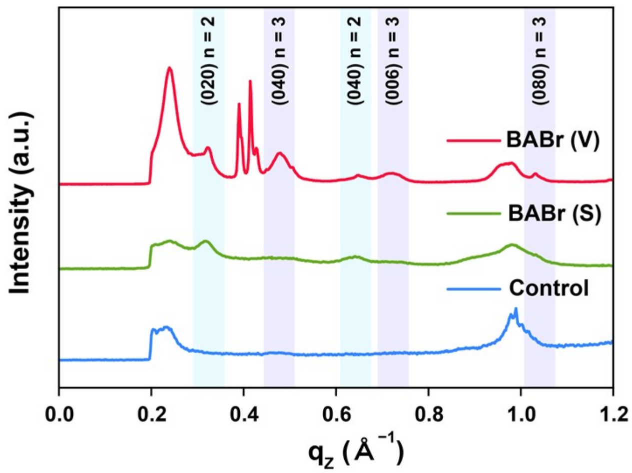

Fig. S1 Signal intensity profiles of GIWAXS patterns along q_z axis.

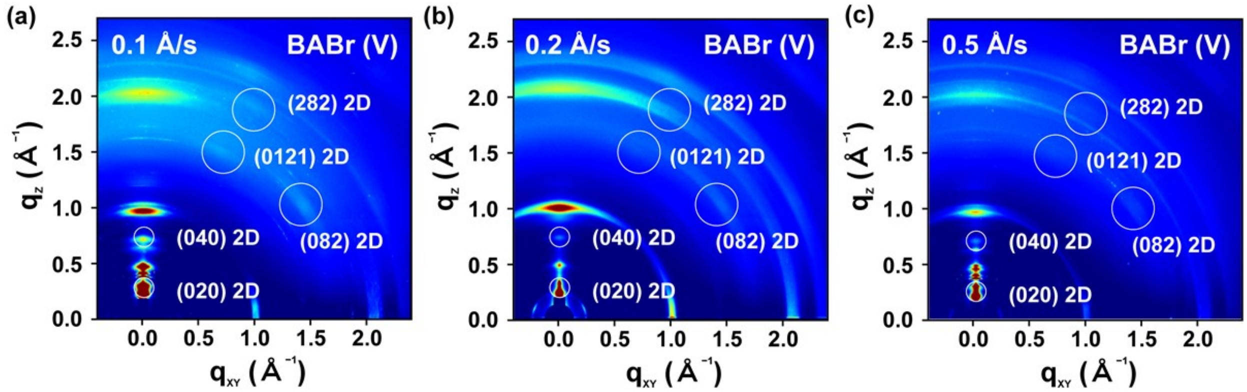

Fig. S2 GIWAXS patterns of BABr (V) films with RP phase perovskite deposition rates of (a) 0.1, (b) 0.2, and (c) 0.5 Å/s.

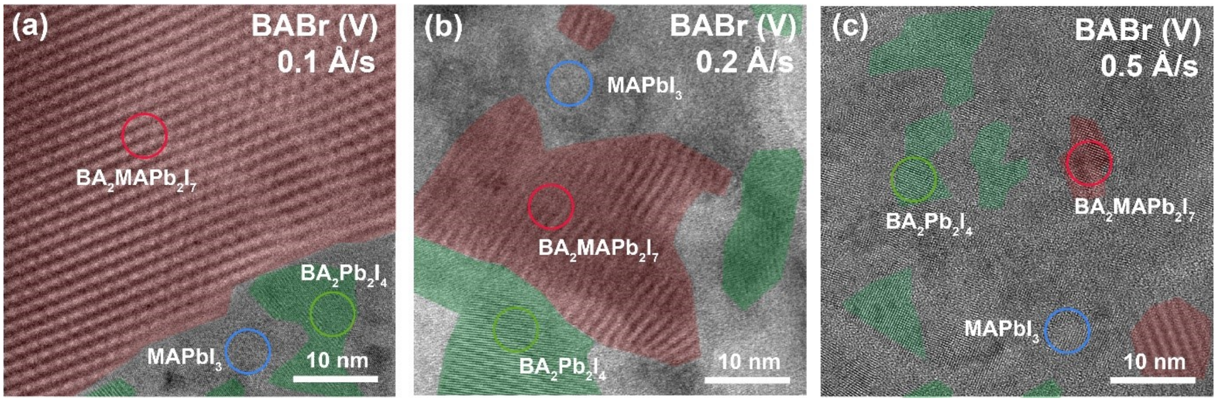

Fig. S3 HRTEM images of BABr (V) films with RP phase perovskite deposition rates of (a) 0.1, (b) 0.2, and (c) 0.5 Å/s.

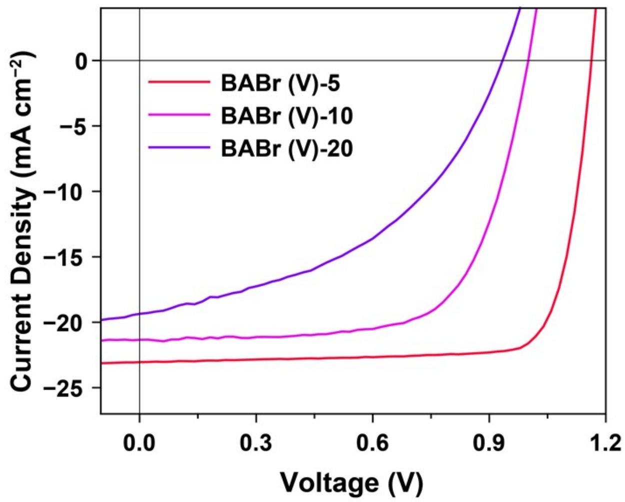

Fig. S4 $J-V$ characteristics of BABr (V) PSCs with different RP perovskite deposition times.

Table S1 Photovoltaic parameters of BABr (V) PSCs with different RP perovskite deposition times.

Perovskite	J_{SC} [mA cm^{-2}]	V_{OC} [V]	FF	PCE [%]
BABr (V)-5	23.0	1.16	0.80	21.4
BABr (V)-10	21.1	1.00	0.66	13.9
BABr (V)-20	18.8	0.94	0.44	7.8

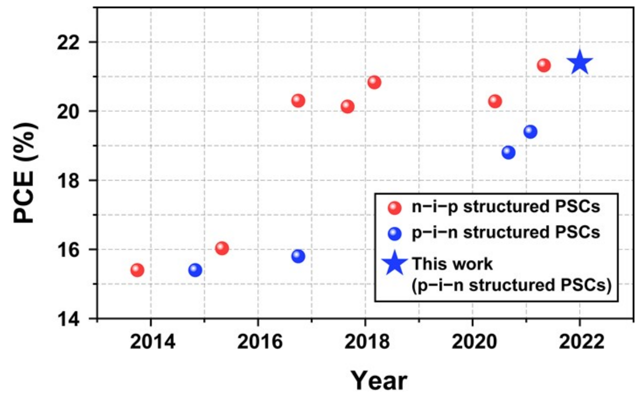

Fig. S5 Comparison of device performance for PSCs with vacuum-deposited perovskite active layer reported in literature.

Table S2 Photovoltaic parameters of PSCs with vacuum-deposited perovskite active layer reported in literature.

Year	Structure of PSCs	J_{SC} [mA cm^{-2}]	V_{OC} [V]	FF	PCE [%]	Ref
2013	n–i–p	21.5	1.07	0.67	15.4	[1]
2014	p–i–n	20.9	1.02	0.72	15.4	[2]
2015	n–i–p	22.3	1.00	0.72	16.0	[3]
2016	n–i–p	22.1	1.14	0.81	20.3	[4]
2016	p–i–n	20.0	1.08	0.73	15.8	[5]
2017	n–i–p	23.2	1.10	0.79	20.1	[6]
2018	n–i–p	21.9	1.16	0.82	20.8	[7]
2020	p–i–n	22.6	1.09	0.76	18.8	[7]
2020	n–i–p	23.3	1.12	0.78	20.3	[8]
2021	p–i–n	23.1	1.09	0.77	19.4	[9]
2021	n–i–p	24.9	1.11	0.77	21.3	[10]
2022	p–i–n	23.0	1.16	0.80	21.4	This work

Table S3 Fitted TRPL parameters for perovskite films with passivation layer.

Perovskite	τ_1 [ns]	Fraction 1 [%]	τ_2 [ns]	Fraction 2 [%]
Control	5.2	62	70.5	38
BABr (S)	3.1	71	33.8	29
BABr (V)	2.7	77	25.7	23

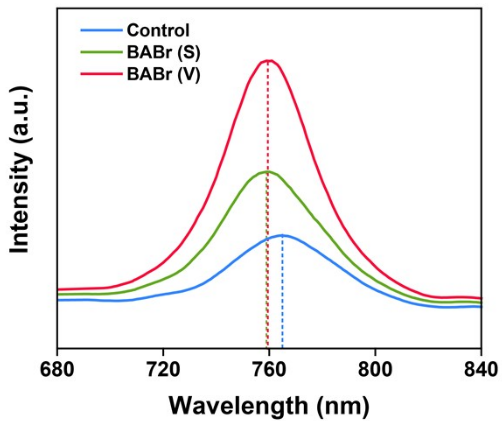

Fig. S6 Steady-state photoluminescence spectra of perovskite films with RP phase perovskite passivation layer.

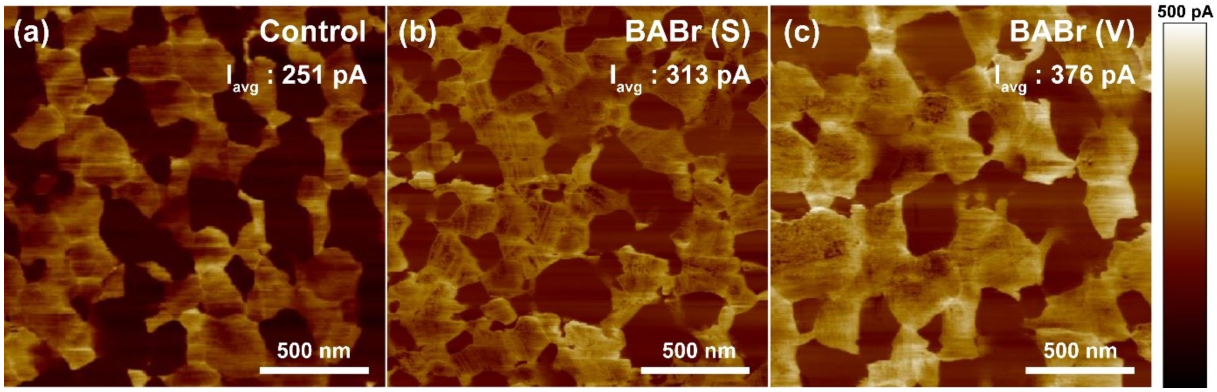

Fig. S7 Conductive AFM images of (a) control, (b) BABr (S), and (c) BABr (V) films.

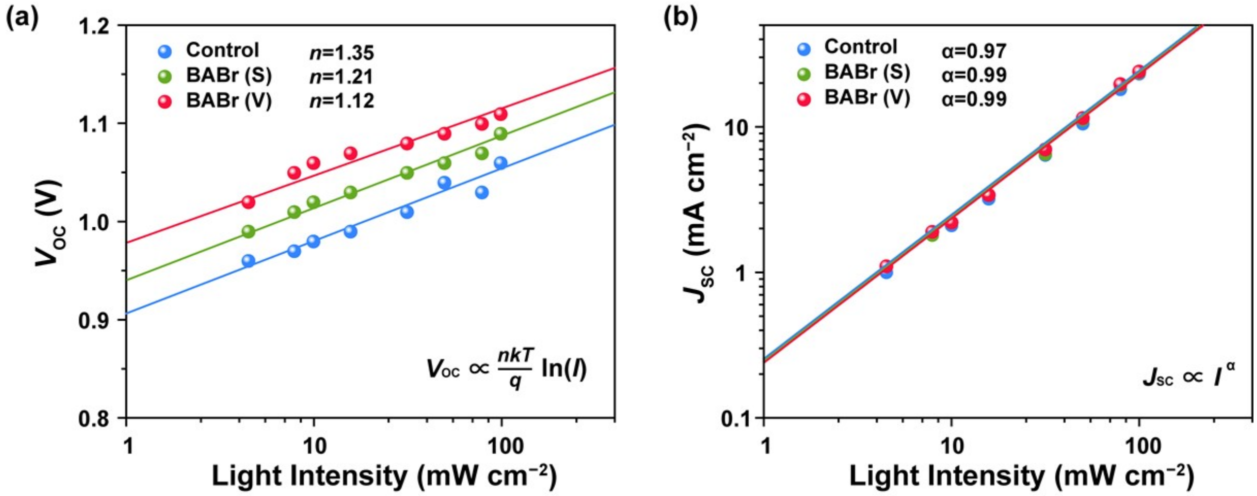

Fig. S8 Light-intensity-dependent (a) V_{OC} and (b) J_{SC} profiles for PSCs with RP phase perovskite passivation layer.

Table S4 Hole and electron trap density and carrier mobility values obtained by space-charge limited current analysis.

Perovskite	N_{th} [cm^{-3}]	N_{te} [cm^{-3}]	μ_h [$cm^2 V^{-1} s^{-1}$]	μ_e [$cm^2 V^{-1} s^{-1}$]
Control	1.86×10^{16}	5.44×10^{15}	1.2×10^{-4}	8.2×10^{-4}
BABr (S)	1.31×10^{16}	3.74×10^{15}	8.6×10^{-4}	1.2×10^{-3}
BABr (V)	1.11×10^{16}	3.33×10^{15}	1.0×10^{-3}	1.4×10^{-3}

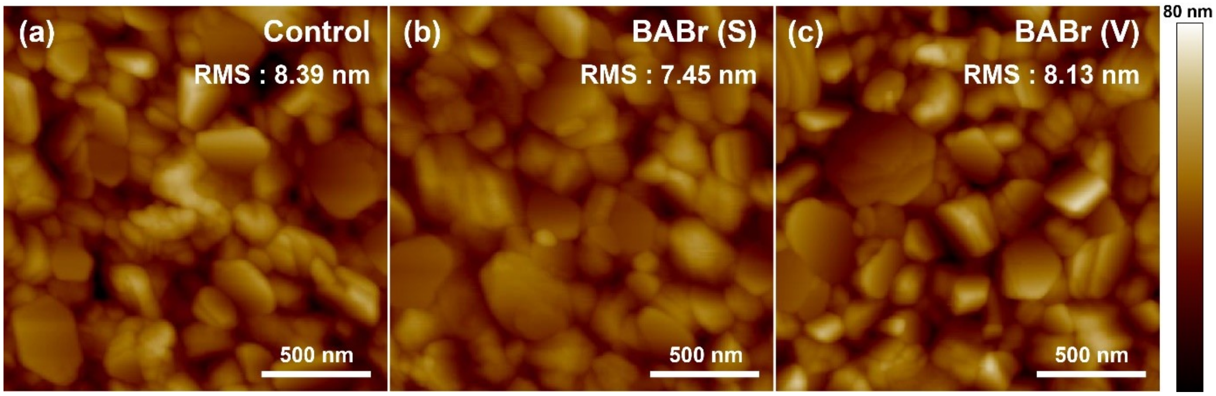

Fig. S9 AFM topography images of (a) control, (b) BABr (S), and (c) BABr (V) films.

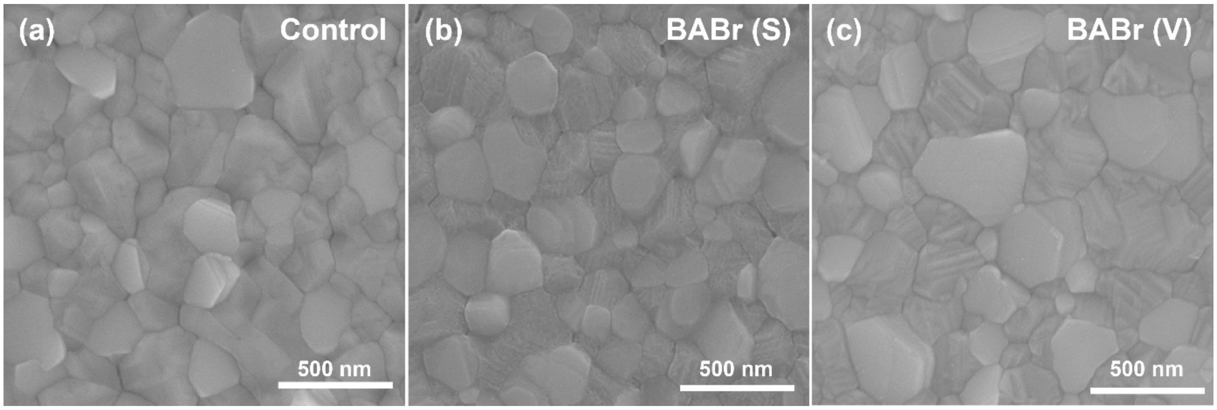

Fig. S10 Top-view SEM images of (a) control, (b) BABr (S), and (c) BABr (V) films.

References

1. M. Liu, M. B. Johnston, H. J. Snaith, *Nature* **2013**, 501, 395–398.
2. C. W. Chen, H. W. Kang, S. Y. Hsiao, P. F. Yang, K. M. Chiang, H. W. Lin, *Adv. Mater*. **2014**, 26, 6647–6652.
3. D. Yang, Z. Yang, W. Qin, Y. Zhang, S. F. Liu, C. Li, *J. Mater. Chem. A* **2015**, 3, 9401–9405.
4. C. Momblona, L. Gil-Escrig, E. Bandiello, E. M. Hutter, M. Sessolo, K. Lederer, J. Blochwitz-Nimoth, H. J. Bolink, *Energy Environ. Sci.* **2016**, 9, 3456–3463.
5. X. Zhu, D. Yang, R. Yang, B. Yang, Z. Yang, X. Ren, J. Zhang, J. Niu, J. Feng, S. Liu, *Nanoscale* **2017**, 9, 12316–12323.
6. D. Pérez-Del-Rey, P. P. Boix, M. Sessolo, A. Hadipour, H. J. Bolink, *J. Phys. Chem. Lett.* **2018**, 9, 1041–1046.
7. L. Gil-Escrig, C. Dreessen, I. C. Kaya, B.-S. Kim, F. Palazon, M. Sessolo, H. J. Bolink, *ACS Energy Lett.* **2020**, 5, 3053–3061.
8. J. Li, H. Wang, X. Y. Chin, H. A. Dewi, K. Vergeer, T. W. Goh, J. W. M. Lim, J. H. Lew, K. P. Loh, C. Soci, T. C. Sum, H. J. Bolink, N. Mathews, S. Mhaisalkar, A. Bruno, *Joule* **2020**, 4, 1035–1053.
9. M. M. Tavakoli, R. Tavakoli, *Phys. Status Solidi-RRL* **2020**, 15, 2000449.
10. J. Feng, Y. Jiao, H. Wang, X. Zhu, Y. Sun, M. Du, Y. Cao, D. Yang, S. Liu, *Energy Environ. Sci.* **2021**, 14, 3035–3045.